University of Huddersfield Repository

Zhao, Xin, Lucas, Gary and Pradhan, Suman

Signal Processing method in using four-sensor probe for measuring the velocity vector of air-liquid two phase flow

Original Citation

Zhao, Xin, Lucas, Gary and Pradhan, Suman (2009) Signal Processing method in using four-sensor probe for measuring the velocity vector of air-liquid two phase flow. Journal of the Japanese Society of Experimental Mechanics (JSEM), 9. pp. 19-24.

This version is available at https://eprints.hud.ac.uk/id/eprint/6997/

Signal Processing Method in using Four-sensor Probe for Measuring the Velocity Vector of Air-liquid Two-phase Flow

Xin ZHAO[1], Gary LUCAS[1] and S. PRADHAN[1]

[1] School of Computing and Engineering University of Huddersfield, Huddersfield HD1 3DH, UK

Abstract
This paper describes a new design of a local four-sensor probe which was used to measure the local velocity vector of the dispersed phase in a bubbly gas-liquid two phase flow. Based on the four-sensor probe signals, a new signal processing technique was also introduced. Reference data was obtained using high speed cameras to determine the optimum value for the threshold voltages relevant to the output signals from the four sensors on the probe. Groups of signals from the four sensors that were generated by the same bubble were identified but the signals from some bubbles were ignored by the signal processing scheme. After using the signal processing technique, the results have been improved compared with the results without the signal processing technique.

1. Introduction
Measurement of the volumetric flow rate of each of the flowing components in multiphase flow is often required. In recent years, there has been an increase in the level of interest shown in making such measurements. Many dual and four probe sensors were built to measure the flow velocity in multiphase flow [1-7]. This has relevance to many applications e.g. the oil industries, chemical and nuclear power industries. For example, the measurement of the flow rate of each component is required for production logging applications, where it may be necessary to measure the flow rates of oil and water down hole in vertical and inclined oil-water wells.

In this paper, a novel kind of conductive four sensor probe and the associated mathematical model are introduced. The probe is used to measure the velocity vectors of gas bubbles, which form the dispersed phase in a bubbly air-water two-phase flow. One of the main considerations is the choice of an appropriate threshold value for the output signal from each of the four sensors, corresponding to the times when the surface of the bubble is in contact with the relevant sensor. The correct choices for the threshold values for each sensor enable the time delays relevant to the mathematical model associated with the four sensor probe technique to be calculated more accurately (section 2). Because different bubbles contact the probe in different ways, generating different types of signals, it is also important to develop a signal processing method to determine which segments of the signals from the four sensors were caused by the same bubble. Finally, the signal processing technique must eliminate bubbles whose surface does not unambiguously come into contact twice with each of the fours sensors in the probe.

2. Four-sensor Probe and the Mathematical Model
The four sensor probe was made from four PTFE coated needles of 0.15mm outer diameter, with the PTFE removed from the very tip of each needle to allow electrical contact with the multiphase flow. To position the needles, and to increase the probability that particles of the dispersed phase make contact with lead sensor before contacting the other sensors, a centrally drilled 2mm diameter ceramic guide was used to mount the needles. This probe design is shown schematically in figure 1 and a photograph showing the relative positions of the sensors is given in figure 3. The geometrical arrangement of the sensors in the probe was an improvement on previous work [2] and was intended to increase the number of bubbles striking the lead sensor (0) which also strike all of the three rear sensors (1, 2 and 3). The probe co-ordinate system is shown in figure 2. Also shown in figure 2 is the velocity vector **V** of an approaching bubble relative to the probe co-ordinate system.
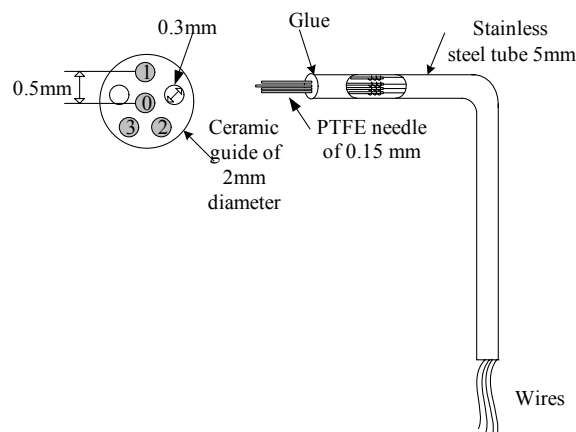
Fig. 1 Schematic of four-sensor probe

Figure 3 shows an image of the probe viewed 'end on' under a microscope in order to measure the x and y co-ordinates of sensors 1, 2 and 3 with respect to the front sensor 0 (which is located in the middle of the probe). 'Red' denotes sensor 1, 'Blue' denotes sensor 2, 'Green' denotes sensor 3 and the sensor denotes 'Black' is the lead sensor '0'. The two thin lines crossing each other are the x and y axes of the probe. For the experiments described in this paper the z co-ordinate of each of the three rear sensors was 1mm.

The stainless steel tube forming the probe body was used as common earth electrode for the four sensors. The

conductance at each sensor was measured using a circuit based on the design given in figure 4, in which the sensor resistance R_s between the tip of the relevant sensor and the stainless steel tube. The water resistance is relatively small compared to R_{ref} (which has a typical value of 1.5M). When the tip of the acupuncture needle is immersed in an air bubble, the quantity R_{ref}/R_s approaches V_{in}. So the signals of the sensors fall down from V_{in} when each sensor is alternately immersed in water and air.
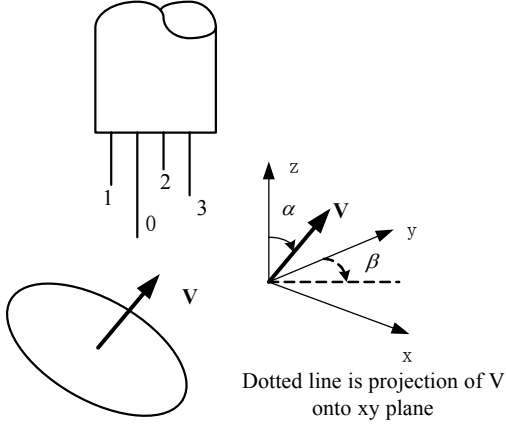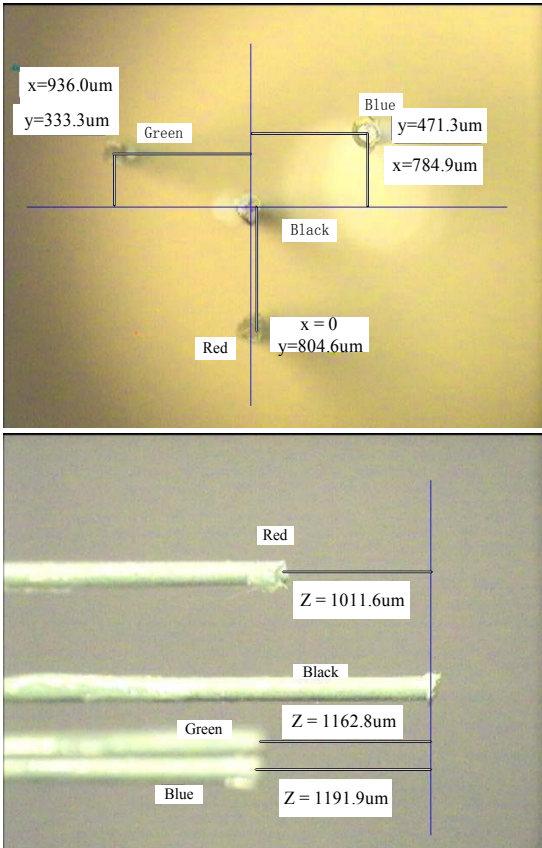

Fig.2 Probe coordinate system.

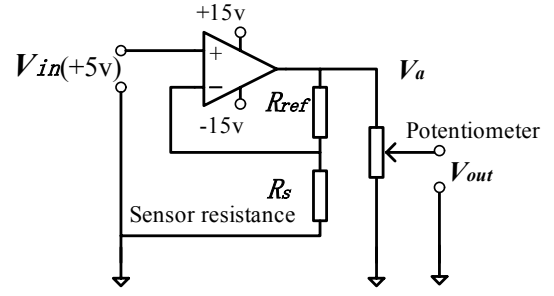Fig.3 The 4-sensor probe viewed under a microscope

Fig.4 Circuit diagram used with each of the four sensors

Based on the probe signals and the definition of the probe coordinate system (Fig. 2) we can set up a mathematical model to calculate the bubble vector velocity [2]. In this model, three independent equations (1, 2 and 3 below) in v (bubble velocity magnitude), α (polar angle of bubble velocity vector) and β (azimuthal angle of bubble velocity vector) are derived.

$$\frac{v\delta t_{11}}{2} = x_1 \sin\alpha \sin\beta + y_1 \sin\alpha \cos\beta + z_1 \cos\alpha \qquad (1)$$

$$\frac{v\delta t_{22}}{2} = x_2 \sin\alpha \sin\beta + y_2 \sin\alpha \cos\beta + z_2 \cos\alpha \qquad (2)$$

$$\frac{v\delta t_{33}}{2} = x_3 \sin\alpha \sin\beta + y_3 \sin\alpha \cos\beta + z_3 \cos\alpha \qquad (3)$$

Where x_i, y_i, z_i represent the position of the ith rear sensor (i=1, 2, 3) in the coordinate system of the four-sensor probe and where δt_{ii} (i=1, 2, 3) is defined as

$$\delta t_{ii} = \delta t_{ia} + \delta t_{ib} - \delta t_{0b} \qquad (4)$$

where δt_{ia} is the time interval between the first contact of the bubble surface with front sensor 0 and the first contact of the bubble surface with the ith rear sensor, δt_{ib} is the time interval between the first contact of the bubble surface with front sensor 0 and the last contact of the bubble surface with the ith rear sensor, and δt_{0b} is the time between the first and last contacts of the bubble surface with the front sensor.

By solving equations 1, 2 and 3 simultaneously the following expressions for $\tan\beta$ and $\tan\alpha$ are obtained.

$$\tan\beta = \frac{\left(\frac{z_1}{\delta t_{11}} - \frac{z_2}{\delta t_{22}}\right)\left(\frac{y_1}{\delta t_{11}} - \frac{y_3}{\delta t_{33}}\right) - \left(\frac{z_1}{\delta t_{11}} - \frac{z_3}{\delta t_{33}}\right)\left(\frac{y_1}{\delta t_{11}} - \frac{y_2}{\delta t_{22}}\right)}{\left(\frac{z_1}{\delta t_{11}} - \frac{z_3}{\delta t_{33}}\right)\left(\frac{x_1}{\delta t_{11}} - \frac{x_2}{\delta t_{22}}\right) - \left(\frac{z_1}{\delta t_{11}} - \frac{z_2}{\delta t_{22}}\right)\left(\frac{x_1}{\delta t_{11}} - \frac{x_3}{\delta t_{33}}\right)} \qquad (5)$$

$$\tan\alpha = \frac{\frac{z_1}{\delta t_{11}} - \frac{z_2}{\delta t_{22}}}{\left(\frac{x_2}{\delta t_{22}} - \frac{x_1}{\delta t_{11}}\right)\sin\beta + \left(\frac{y_2}{\delta t_{22}} - \frac{y_1}{\delta t_{11}}\right)\cos\beta} \qquad (6)$$

To obtain the magnitude and direction of the bubble velocity, β is calculated using equation 5 in conjunction with the measured time intervals δt_{ii} and the known sensor coordinates x_i, y_i, z_i. Next, α is calculated using equation

6. Finally, v is calculated using any one of equations 1, 2 and 3.

3. Signal Processing Method

Figure 5 shows the raw signals from the four-sensor probe as the sensors contact a particular bubble. From the mathematical model, the time intervals have to be calculated from these probe signals. Therefore a suitable signal processing technique is needed to extract the required information from the raw signals. Some techniques will be presented in this section.

Firstly the output signals from the four sensor conductivity probe differ from an ideal square-wave so if we choose different threshold voltage values we will generate different time intervals δt_{ii}.

Secondly the bubble-probe interaction is complex, some bubbles only touch some of the four sensors and so it is necessary to find out which of the four 'square-wave' signals (Fig. 5) are caused by the same bubble (this can be particularly difficult when bubble velocity and the gas volume fraction are quite high).

Thirdly, in any flow condition, not all the bubbles unambiguously contact each sensor twice, leading to errors in the estimates of δt_{ii}. Consequently, such bubbles should be ignored in order to improve the accuracy of the calculation.
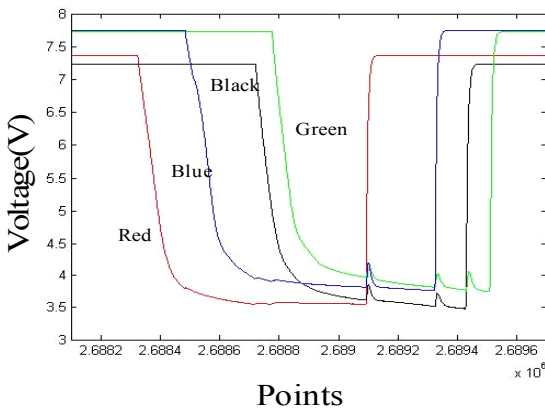

Fig.5 The raw signals of the four-sensor probe

3.1 Choice of Threshold Voltage Value

From the raw signals (figure 5), we can see that the fall, and rise, in the voltage signals due to the passage of a bubble are not vertical but have a well defined slope. There is therefore uncertainty as to the values of output voltage corresponding to the times at which the bubble surface makes first and last contacts with the sensor. This may be because there is a small reduction in the sensor conductance just before the bubble actually touches the sensor, due to the bubble partially blocking the flow of electrical current through the water from the sensor tip to the earthed probe body. For a similar reason the sensor conductance may not return to its maximum value until a short time after the bubble has ceased to be in contact with the sensor. In [2], the transient response of the four-sensor probe has been

analysed to find out that the relative insensitivity of these time intervals to the choice of the threshold voltages value.

In order investigate the effect of different threshold voltage values on the velocity vector measurement the following work was undertaken *[NB threshold voltage is defined in this paper as a reduction δV in the output from a sensor compared to the output voltage when the sensor is immersed in water only. For a given probe the same threshold voltage is applied to all four sensors]*. A water tank of size 100mmx100mm cross sectional area and 750mm high was constructed from 6mm thick perspex sheets. A pressurized air supply was used to inject air bubbles into the base of the tank via a 5mm diameter stainless steel tube (Fig. 6). The air flow rate was controlled using a manual valve. For the experiments described in this paper the bubbles were approximately oblate spheroidal in shape with a 5mm-6mm major axis. The whole system is shown in Figure 6.

A high speed camera system was used to obtain a reference measurement of the rise velocity of the bubbles in the tank. A tank coordinate system (X,Y,Z) can be defined in which Z is in the vertically upward direction. A 250 frames per second high speed camera was used to measure the bubble velocity in the Z direction. We may say that the velocity of the bubbles in the Z direction can be assumed as a constant when the water is stable and the pressure is a constant if we ignore any minor changes in the water temperature.
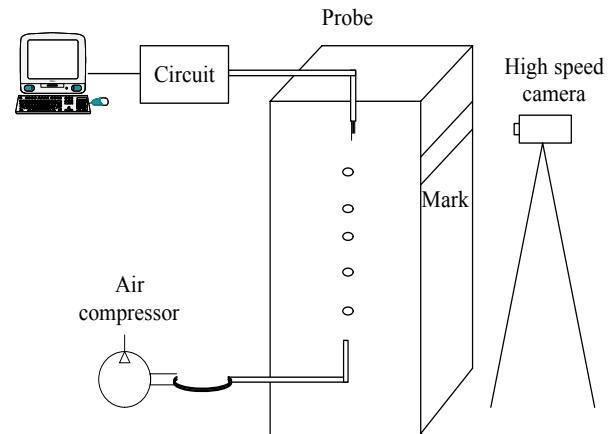
Fig.6 the tank measure system

Two lines separated by a distance of 23mm (in the Z direction) were drawn on the wall of the tank and the high speed camera was used to record the time interval for a given bubble to pass from the first to the second mark. The time interval between successive frames from the camera is equal to 0.004s. Using video processing software, it was possible to count the numbers of the frames for a given bubble to pass between the two lines. The mean reference velocity $v_{z,ref}$ of the bubbles in the 'Z' direction is then given by

$$v_{z,ref} = \frac{23 \times 10^{-3}}{\overline{N}_f \times 0.004} \qquad (7)$$

where $\overline{N}_f$ is the mean number of the frames that the bubbles take to pass the two lines. For all of the experiments described in this paper undertaken using the water tank in Fig. 6 the mean value of the bubble velocity in the Z direction was 0.24m/s.

Different threshold voltage values were used to measure the velocity component of the bubble in the Z direction using the probe signals and the mathematical model in section 2 (NB this is straightforward when the z axis of the probe coordinate system is in the Z direction, but requires the use of mathematical transformations when the z axis of the probe is inclined with respect to the Z axis of the tank [3]). The threshold voltage value δV was varied from 0.2V to 2.0V in 0.1V increments. The velocity of the bubble in the Z direction as measured by the probe is shown in figure 7. From Figure 7, for the different threshold voltage values, the velocities of the bubbles in the 'Z' direction are very close to the reference value 0.24m/s. In fact the mean value is 0.248m/s and the standard deviation is 0.00128m/s. Varying the threshold voltage from 0.2V to 1.5V makes very little difference to the calculated probe velocity in the Z direction. [NB another possible method for choosing the threshold voltage is based on a comparison of the mean local volume fraction measured by the probe with the local volume fraction measured using an alternative technique (such as a differential pressure measurement) [2]]. From the results described above it is believed that the relative insensitivity of the measured velocity in the Z direction to the choice of threshold voltage is a major advantage of the probing technique described in this paper.
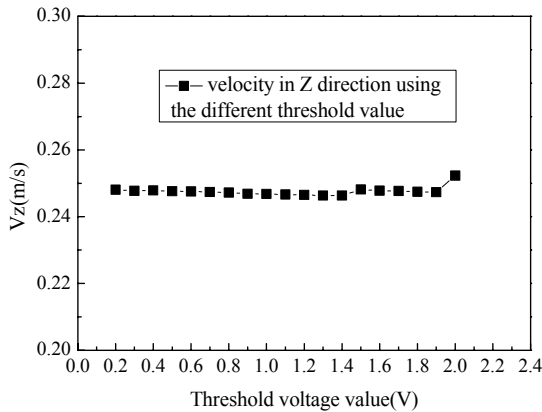

Fig .7 The velocity of the bubble in the Z direction using the different threshold voltage values

Additional experiments were also undertaken in the 80mm i.d. perspex test section of an air-water flow loop [2] (see section 4.2) For these experiments, the axial velocity of the water in which the bubbles travel could be varied. The conclusions regarding the insensitivity of the technique to the threshold voltage, obtained from the tank data, were assumed to apply to the experiments carried out in the flow loop.

3.2 Signal Processing Method

The probe dimensions x_i, y_i, z_i were measured using a microscope with a digital imaging attachment that had an overall accuracy of about $\pm 1\mu m$. To measure the time intervals δt_{ia} and δt_{ib} (section 2) a data acquisition system with a sampling frequency higher than 40Khz is used. This is especially important when the bubble's velocity higher than 0.5m/s. In the experiments described in this paper, a high speed data acquisition card (DAQ2006 ADLink Ltd.) was used to collect the probe signals with a sampling frequency 80Khz.

In the experiments, each bubble is expected to touch sensor 0 first and it then touches the other three rear sensors. The following signal processing criteria were used to ensure that the group of the sensor signals from which δt_{ia} and δt_{ib} were determined were all produced by the same bubble.

1. The first falling edge in the group must be the signal from sensor 0

2. From the first falling edge of sensor 0 to the last rising edge of the group, the time interval should be smaller than a threshold time value which is dependent upon the bubble velocity.

3. Every sensor signal within the group must have only one falling edge and one rising edge.

In the previous work [1], it is mentioned that if a bubble touches the front sensor then there is a high chance that its surface will touch the other three sensors twice. However, this depends upon the relative sizes of the frontal area of the probe and the bubble. Consequently, under some circumstances, the bubble surface will not touch all of the four sensors twice e.g. in the figure 8 (b) which shows the same bubble at three different positions in its trajectory.

Let us suppose that a group of signals satisfies the three criteria mentioned above but was still generated by the two different bubbles. It is possible that the first bubble touches sensor 0 and one or two of the other rear sensors and a second bubble touches the remaining rear sensor. However, if the distance between the sensor 0 and the other three rear sensors is not very great (normally around 1 to 1.5mm for the probes used in this investigation) this eventuality is extremely unlikely.
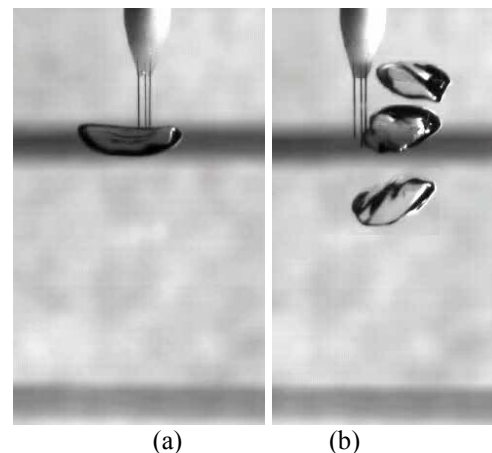

(a)   (b)
Fig. 8 bubbles touch the probe
(a) the bubble touch all of the four sensors
(b) the bubble does not touch some of the sensors

From the criteria given above the bubbles whose surfaces touch each of the four sensors twice can be determined. Most of these bubbles touch the sensors close to the bubble centre but some bubbles may touch a sensor close to the bubble edge. Such contacts give rise to ambiguous signals and so are ignored.

Some such ambiguous signals are shown in figure 9. Here, two kinds signal that should be ignored are illustrated.
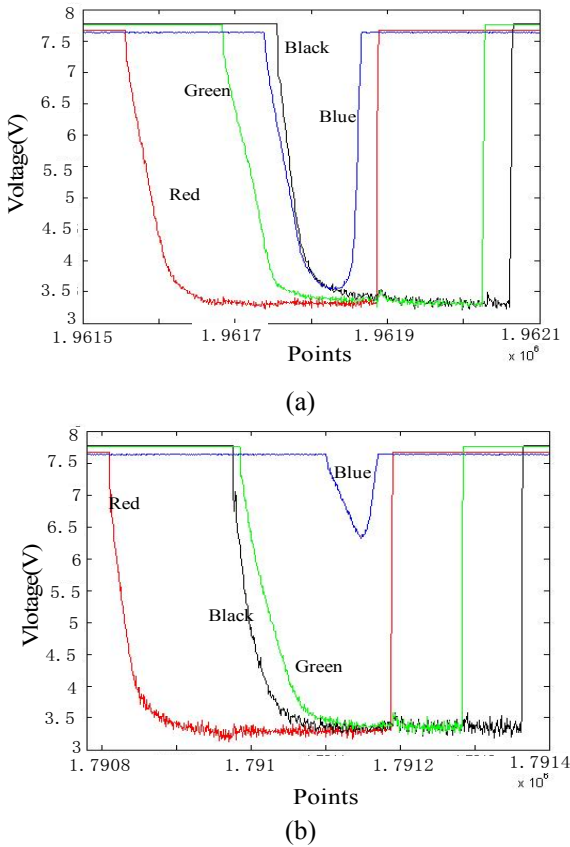

(a)

(b)

Fig. 9 Two kinds of the ambiguous signals

In Figure 9(a) the duration of the blue sensor signal, from the first touch to the second touch, is much shorter than the signals from the other three sensors which means that the bubble touched the sensor (associated with the blue signal) close to the edge of the bubble. In Fig. 9(b), (for a different bubble) the voltage drop from the sensor associated with the blue signal is much smaller than for other three sensors, suggesting that the bubble is only grazing the probe surface.

4 Test Results
For the flow conditions investigated in the test tank the gas bubbles were 5-6mm in diameter and the typical bubble Weber number was about 15. For the flow loop experiments the the gas bubbles were about 9mm in diameter and the typical bubble Weber Number was about 25. For both sets of experiments the four sensors in the probe readily penetrated the gas bubbles.

4.1 Tank Test Results
In the tank coordinate system, the origin is coincident with the position of the lead sensor whilst the z-axis is parallel to the axis of the probe. The x and y axes of the tank coordinate system are chosen arbitrarily but are orthogonal

to each other and to the z-axis. For air bubbles in water it is impractical to attempt to change the direction of the air bubbles, however it is possible to change the direction of the bubble velocity vector relative to the probe coordinate system by tilting and rotating the probe as described in [2]. In this section the quantities α_{ref} and β_{ref} respectively represent reference values of the polar and azimuthal angles that the bubbles make with the probe after it has been tilted and rotated relative to the tank coordinate system. A reference value v_{ref} for the bubble velocity magnitude was obtained using a high speed camera.

For each test undertaken, data was obtained from approximately 30 individual bubbles. After applying the signal processing method described above, the mean value for δt_{ii} (i=1,2,3) was input to the mathematical model in section 2 to calculate bubble velocity vector. The results from the tank test after using the signal processing method is shown in table 1.

Table1 values of polar angle, azimuthal angle and velocity magnitude measured by the probe and reference values for these quantities in the tank

	α_{ref}	β_{ref}	v_{ref}	α_{meas}	β_{meas}	v_{meas}
test	(deg)	(deg)	(ms^{-1})	(deg)	(deg)	(ms^{-1})
1	0	N/A	0.38	4.44	N/A	0.37
2	0	N/A	0.38	7.50	N/A	0.38
3	0	N/A	0.38	2.73	N/A	0.41
4	10	360	0.41	9.01	337.66	0.39
5	10	90	0.41	9.98	82.04	0.44
6	10	180	0.41	6.13	177.65	0.42
7	20	0	0.35	22.41	7.27	0.36
8	20	0	0.35	20.49	16.44	0.36
9	20	180	0.35	19.17	188.31	0.33

The mean absolute errors of $\bar{\varepsilon}_{abs,\alpha}$ and $\bar{\varepsilon}_{abs,\beta}$ in degrees are 1.32º and -0.10º respectively, the relative error of the magnitude of v is less than 7%.

4.2 Air-water Flow LoopTest Results
Using the four-sensor probe, the bubble velocity vector was measured also on the air-water two-phase flow loop, with which a 2.5 m long, 80 mm internal diameter, transparent, vertical test section. Water was pumped into the base of the working section via a turbine meter which enabled the water volumetric flow rate to be measured. Air was pumped into the working section via a series of 1 mm diameter holes, equispaced around the circumference of the base of the working section, giving rise to oblate spheroidal air bubbles with major axes that were typically about 5 mm to 8 mm long. The mass flow rate of the air was measured before it entered the working section using a thermal mass flow meter. A high speed camera was again used to measure the velocity reference v_{ref} of the bubbles. Again, the quantities α_{ref} and β_{ref} respectively represent reference values of the polar and azimuthal angles that the bubbles make with the probe after it was tilted and rotated relative to the

coordinate system of the flow loop test section. The reference value v_{ref} of the bubble velocity magnitude was varied by changing the water flow rate. The reference polar angle α_{ref} was set at the three different angles of 34, 21 and 14 degrees whilst the reference azimuthal angle β_{ref} was kept constant at 0 degrees (equivalent to 360degreea).

Table 2 shows the measured results using the four sensor probe before and after application of the signal processing method described in section 3

.	v_{ref} m/s	α_{ref}	β_{ref}	BS v m/s	BS α	BS β	AS v m/s	AS α	AS β
1	0.34	34	360	0.39	16. 9	275.3	0.41	31.3	334.4
2	0.39	34	360	0.41	28.8	337.1	0.38	30.2	340.1
3	0.49	34	360	0.50	32.6	327.7	0.48	34.8	323.6
4	0.52	34	360	0.47	23.5	258.0	0.56	31.9	340.5
5	0.34	21	360	0.41	13.5	296.8	0.42	23.3	332.8
6	0.34	21	360	0.43	22.2	333.9	0.42	21.7	332.8
7	0.49	21	360	0.44	31.6	282.2	0.49	19.86	320.9
8	0.52	21	360	0.45	30.33	25.41	0.56	26.30	346.7
9	0.34	14	360	0.44	11.06	316.68	0.43	13.58	305.4
10	0.39	14	360	0.44	17.26	305.40	0.45	15.13	330.1
11	0.25	14	360	0.29	3.42	85.54	0.29	13.65	266.7
12	0.25	14	360	0.31	9.52	325.23	0.30	15.36	300.1

In the table2, 'BS' and 'AS' were respectively used to represent results obtained before and after application of the signals processing method. For each test shown in Table 2 measurements were obtained from approximately 100 bubbles of which approximately 10% were discarded when the signal processing scheme was applied.

With reference to Table 2, comparison of the calculated results with and without the signals processing method shows that the signal processing method yields results for α , β and v which in general are much closer to the reference values for these quantities. The mean errors for the calculated values of these quantities prior to signal processing are: for v mean error equals 15.4%; for α mean absolute error equals 7º ; for β mean absolute error equals 54.4º. The mean errors after signal processing are: for v mean error equals 13.5%; for α mean absolute error equals 1.8º; for β mean error equals 37.2º.

5. Conclusions and Further Work
In this paper, a new design for a four-sensor probe and the associated mathematical model have been introduced. A new scheme for processing the probe output signals prior to application of the mathematical model has also been introduced.

For the signal processing method, it was found out that the results are relatively insensitive to the threshold voltage value. A series of criteria were set up to ensure that the group of signals from which the time intervals δt_{ii} (from which the bubble velocity vector is calculated) were all generated by the same bubble.

The signal processing method ignores some bubbles which touch the probe in an ambiguous manner. From the tests carried out in tank and an air-water two phase flow loop, it was found that the accuracy of the measurement has been

substantially improved by using the signal processing method. It is believed that these results, after signal processing, are amongst the best yet obtained for this type of measurements. Further work will be undertaken into optimising the geometrical arrangement of the needle sensors in the probe to further reduce the remaining errors in the measured values of α and β .

For the results presented in this paper the probe was used to measure the velocity vector of oblate spheroidal bubbles with major axes in the range 5-12mm. It is unlikely that the present probe could measure a bubble with a major axis much smaller than about 3.5mm.

Nomenclature

α	Polar angle	(degrees)
β	Azimuthal angle	(degrees)
v	Velocity magnitude	(m/s)

δt_{ii} δt_{11} δt_{22} δt_{33}
Time delays (s) calculated from the times at which the bubble surface contacts sensors 0, 1, 2 and 3

δt_{ia}, δt_{ib}
Time delays between first bubble contact with sensor 0 and first and last bubble contacts (respectively) with sensor i(s)

α_{ref}	Reference polar angle	(degrees)
β_{ref}	Reference azimuthal angle	(degrees)
v_{ref}	Reference velocity magnitude	(m/s)
α_{meas}	Measured polar angle	(degrees)
β_{meas}	Measured azimuthal angle	(degrees)
v_{meas}	Measured velocity magnitude	(m/s)

References
[1] Mishra, R., Lucas, G.P. and Kieckhoefer, H.: *Meas. Sci. Technol.*, **13** (2002), 1488-1498.

[2] Lucas, G.P. and Mishra R.: *Meas. Sci. Technol.*, **16** (2004), 749-758.

[3] Panagiotopoulos, N. and Lucas, G.P.: *Meas. Sci. Technol.*, **18** (2007), 2563-2569.

[4] Pradhan, S., Lucas, G.P. and Panagiotopoulos, N.: *Researchers Conference University of Huddersfield.* UK (2006).

[5] Hosgett, S. and Ishii, M.: *Nuclear Engineering and Design.*, **175** (1997), 15-24.

[6] Kim, S., Fu, X.Y., Wang, X. and Ishii, M.: *International Journal of Heat and Mass Transfer*, **43** (2000), 4101-4118.

[7] Ishii, M. and Kim, S.: *Nuclear Engineering and Design*, **205** (2001), 123-131.